Dynamic Clustering Regulates Activity of Mechanosensitive Membrane Channels

Alexandru Paraschiv,[1,4] Smitha Hegde,[2] Raman Ganti,[3] Teuta Pilizota,[2] and Anđela Šarić[1,4,*]
[1]Department of Physics and Astronomy, Institute for the Physics of Living Systems University College London, London WC1E 6BT, United Kingdom
[2]Centre for Synthetic and Systems Biology University of Edinburgh, Edinburgh EH9 3FF, United Kingdom
[3]Institute for Medical Engineering and Science Massachusetts Institute of Technology, Cambridge, Massachusetts 02142, USA
[4]MRC Laboratory for Molecular Cell Biology, University College London, London WC1E 6BT, United Kingdom

(Received 20 February 2019; published 31 January 2020)

Experiments have suggested that bacterial mechanosensitive channels separate into 2D clusters, the role of which is unclear. By developing a coarse-grained computer model we find that clustering promotes the channel closure, which is highly dependent on the channel concentration and membrane stress. This behaviour yields a tightly regulated gating system, whereby at high tensions channels gate individually, and at lower tensions the channels spontaneously aggregate and inactivate. We implement this positive feedback into the model for cell volume regulation, and find that the channel clustering protects the cell against excessive loss of cytoplasmic content.

DOI: 10.1103/PhysRevLett.124.048102

Both eukaryotic and prokaryotic cells harbour a phospholipid membrane packed with proteins, which enables the separation of cellular content from the external environment. This physical barrier facilitates the transport of signals and materials between the cell and its environment, thus sustaining life [1]. In addition, membranes of unicellular organisms separate the cell from the outside world, and need to be able to respond quickly and efficiently to sudden changes in the cell's surroundings. A common way the membranes respond to external stimuli is by reorganizing associated macromolecules [2]. A characteristic example of such a behavior are membrane mechanosensitive channels (MSCs), which sense mechanical cues from the cell's surrounding, and are central to senses of hearing, balance, and touch, as well as for maintaining cell osmotic homeostasis [3–5].

The best studied MSCs are those of bacterium *Escherichia coli*, whose role is to protect the cell against sudden drops in the environmental solute concentration, so called hypoosmotic shock [6,7]. Upon hypoosmotic shock, water rushes into the cell, resulting in the cell swelling and increased tension in the bacterial envelope, which contains protein-filled phospholipid membranes and a stiffer material called the cell wall [6,7]. If left unchecked, this pressure can lead to cell death by rupturing the envelope [8,9]. To prevent it, a portfolio of MSC in *E. coli*'s inner membrane act as "pressure release valves" that open nanosized pores at their centers. This enables solute and water efflux, reestablishing desired osmotic pressure inside the cell [10–12]. The channel opening is fast and the overall cell's response is solely regulated by the membrane tension and chemical potential of water and solutes [12].

Bacterial MSCs consist of closely-packed transmembrane helices connected by loops [13,14]. Driven by membrane tension, the helices tilt with respect to one another, creating a space between them (up to 3 nm in diameter) for small solutes to nonselectively pass through [15,16]. Recent experimental studies debate the existence and the role of spontaneous clustering of *E. coli*'s MSC of large conductance [17,18]. Membrane clustering appears to be a common mechanism in cellular signaling, and has been observed for many transmembrane proteins and signaling receptors [19]. Clustering of MSC *in vitro* has been shown to result in nonlinear, collective, gating behavior [17], suggesting that it could tamper with cell's passive response to hypoosmotic shock. However, assessing the extent of MscL clustering via imaging techniques *in vivo* has proven difficult due to the potential artifacts of the MscL tags on the process [18], and opens a need for orthogonal ways to investigate the clustering phenomenon. Here, by developing a minimal computer model of MSCs embedded in a membrane, we investigate the physical mechanisms behind the MSC cluster formation and cooperative gating, and their implications on cell-volume regulation.

Guided by the known structures of various MSCs [13,14,20], we designed a model that captures only the key general features of MSCs—namely that they are built of connected rod-shaped subunits [Fig. 1(a)]. While bacterial MSCs possess varying number of repetitive helical subunits [7], without a loss of generality, we choose to include five subunits connected by springs. Each rod is made of hydrophobic core and two hydrophilic head beads [Fig. 1(a)]. The rods are longer than the membrane thickness to reproduce a hydrophobic mismatch of ∼0.5 nm found in structural studies [13]. The bilayer is described by

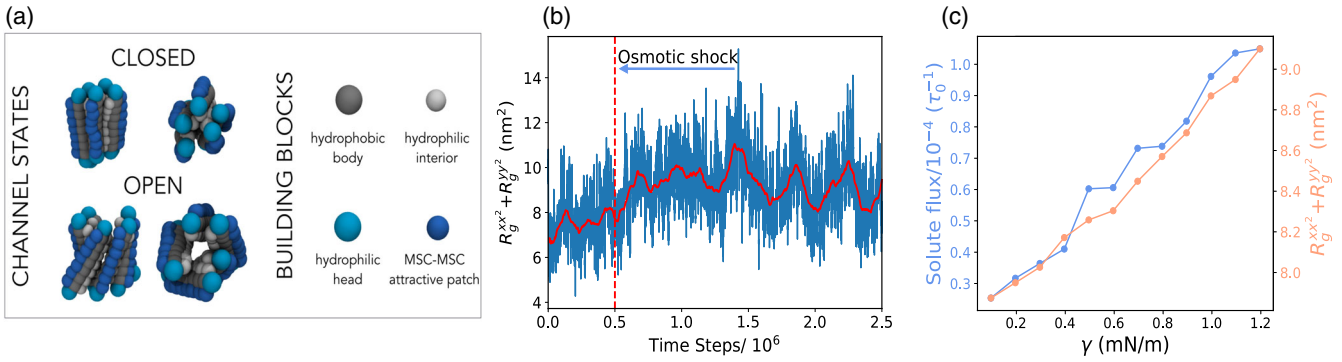

FIG. 1. Single channel properties. (a) MSC is modelled as five rods connected by springs. Each rod consists of hydrophobic (gray) and hydrophilic heads (cyan) and is ∼10 nm long. Channel are lined with hydrophilic beads (silver). Explicit inter-channel attractions can be turned on via a hydrophobic patch (dark blue). Under osmotic shock the MSC naturally opens. (b) Pore size of a single MSC. The vertical red line marks the application of an instantaneous osmotic shock yielding membrane tension of $\gamma = 1.2$ mN/m. The solid red line is the moving time average (window: 10^5 time steps). (c) The variation of the pore size and solute flux though the channel versus membrane tension.

a three-beads-per-lipid model (Figs. S1 and S2 [21]) that reproduces the correct coarse-grained mechanical and dynamical properties of biological membranes [29]. The rod diameter is twice that of a lipid bead and the inner part of the channel is lined with hydrophilic beads to prevent lipids from overflowing inside the channel. Finally, to be able to include direct interprotein attractions, an attractive patch of beads is added on the external side of each rod. Hypoosmotic shock is generated by placing a gas of inert volume-excluded "solute" beads on one side of the membrane. The collisions of the solute beads with the membrane create membrane tension, linearly proportional to the solute concentration difference across the membrane (Fig. S5). For further details see the Supplemental Material [21].

We first investigate the behavior of a single MSC. Application of hypoosmotic shock causes an increase in the membrane tension and area. Since the transmembrane components of the MSC interact attractively with the membrane's hydrophobic layer, they maintain contact with the expanding bilayer, and naturally tilt with respect to one another. This results in the overall lateral expansion of the channel, as shown in Fig. 1 and Video 1. To quantify the channel pore size we measure the in-plane components of the MSC radius of gyration tensor $R_G^{xx^2} + R_G^{yy^2}$ (see the Supplemental Material [21]). We find that the pore size oscillates stochastically, reminiscent of the fluctuations in the flux through MSCs seen in experiments [30]. The application of hypoosmotic shock leads to an immediate increase in the pore size [Fig. 1(b)], allowing for the passage of the solutes and channel gating (Video 2). As shown in Fig. 1(c), the pore size and the solute flux through the pore increase with the shock magnitude. For the purpose of our analysis solely, we chose $\gamma = 0.45$ mN/m as the threshold tension for the pore opening; channels whose pore size is above 8.2 nm^2 we consider as open, while those below we deem as closed [Eq. (S5)].

We now analyze the behavior at multiple MSCs interacting only via volume exclusion and effective membrane-mediated interactions. Figure 2 shows the gating properties of such MSCs as a function of the number of channels in the system. In this case we did not observe any channel clustering and it is evident that each channel behaves independently. Indeed, we find that the membrane-mediated interactions between fluctuating channels in our system are negligible (Fig. S7 [21]). Rigid symmetric inclusions of the same hydrophobic mismatch in our model experience weak attraction of ∼0.5 kT (Fig. S8), in agreement with previous simulation studies [31–33]. Since we did not observe any MSC clustering due to pure membrane-mediated interactions, we chose a top-down strategy. We know that (i) MSC aggregation has been reported *in vitro* [17] and *in vivo* in MSCs labeled with a small covalent dye

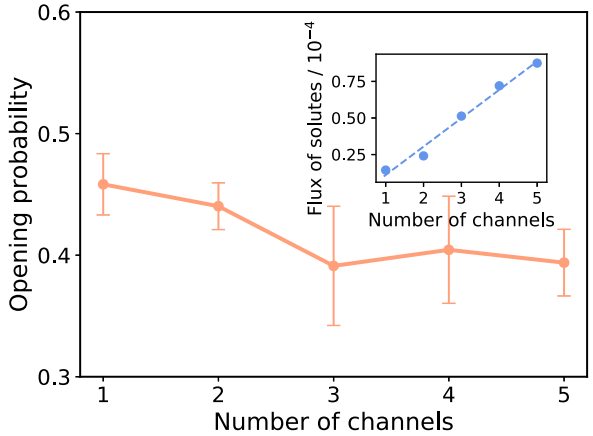

FIG. 2. Multiple channels interacting only via membrane-mediated interactions gate independently. The probability of channel pore opening versus the number of channels present in the system. The error bars correspond to the standard deviation of five different runs. Inset: total flux of solutes through the channels versus the number of channels in the system.

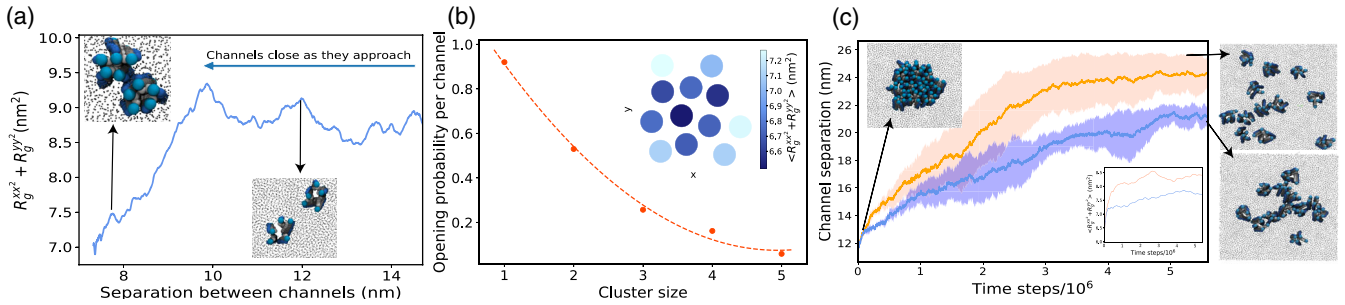

FIG. 3. Channels interacting via explicit attractive interactions gate cooperatively. (a) Average pore size of two MSCs as a function of distance between them ($\gamma = 1.30$ mN/m). (b) Opening probability per channel versus cluster size ($\gamma = 1.70$ mN/m, MSC fraction is 0.16, $\epsilon_{\text{protein-protein}} = 0.9$ kT). The dashed line is a guide to the eye. Inset: The average pore size within a single cluster of 12 MSCs. (c) Upon osmotic shock the average distance between the channels in a cluster increases and is larger for higher membrane tension (orange: $\gamma = 1.70$ mN/m, blue: $\gamma = 0.70$ mN/m). The shading shows a 95% confidence interval of five simulation runs. Far right: Cluster configuration in the last time frame. Inset: MSC opening increases as they disperse.

[18], (ii) direct interprotein interactions, such as polar and electrostatic interactions and packing of small apolar side chains [34–39], can lead to attractions of transmembrane proteins [19]. In addition, local lipid phase separation around the protein can yield effective interprotein attraction and protein aggregation. Therefore, to drive MSC clustering we included weak direct interprotein attractions, which we modelled via an attractive stripe on the outer side of the channel [Fig. 1(a)].

Incorporating weak direct interprotein attraction leads to the assembly of MSCs into small clusters of sizes between 2 and ~15 MSCs, and we now find that the clusters exhibit strong cooperative gating. Figure 3(a) shows how the pore sizes of two attractive channels varies as they approach each other. A sharp decrease in the pore sizes at ~9.5 nm of interchannel separation corresponds to the cooperative closure of individual MSC (Video 3). The reason for this is purely geometrical: two closed channels can achieve larger contact area between them, maximizing their attraction. For multiple channels diffusing in the bilayer we observe aggregation into larger clusters that leads to decreased gating activity per channel, which scales with the cluster size [Fig. 3(b)]. The clusters are dynamic in nature, whereby individual channels within the clusters oscillate between the closed and open states, can move within or leave the cluster, or join another. Since the channel activity depends on the number of neighbors, individual channel activity within a cluster is consequentially inhomogeneous [40]: the channels on the cluster interior will on average gate less than the channels at the cluster rim [inset in Fig. 3(b)].

We now perform a computational experiment to mimic the situation in which a bacterial cell, living under quiescent conditions, encounters a sudden hypoosmotic shock. We start our simulation with a membrane that contains channels all aggregated into a single cluster. We then applied a sudden tension of 1.7 mN/m, and monitored the system in time. As a control, the same simulation was repeated at smaller tension [Figs. 3(c), S11]. We find that the high magnitude shock breaks up the cluster into individual channels, switching the system from the clustered to the dispersed state (Videos 4 and 5). Driven by membrane tension, the MSC structural change from upright to tilted helices leads to less surface-to-surface contact between MSCs and destabilization of the cluster. Such isolated channels gate more easily [inset in Fig. 3(c)], enabling efficient gating at high membrane tensions, when it is needed most. On the contrary, at low tensions the channels remain in a cluster, albeit the cluster shape dynamically elongates [Fig. 3(c)]. The effect will be present as long as the attractions are relatively weak, within the range of physiological interprotein attractions [34–39], such that the channels can change their conformation in the cluster and retain their functionality. Figure S9 [21] demonstrates that the effect persists across a range of chosen interprotein attractions (0 to ~10 kT), while Fig. S15 shows that the result is not sensitive to the particular choice of the attractive patch geometry.

These findings suggest that the spontaneous formation of MSC clusters enables an additional level of control over their gating and signal transduction. This control is implemented in the system in a passive way, hardwired in the system's geometrical properties. On average, single channels are more closed at low membrane tensions, making the channels more aggregation prone, which in turn packs MSCs into clusters and further deactivates their gating. When the cell encounters a hypoosmotic shock, the membrane tension increases and channels open, making them less aggregation prone, which results in spontaneous dispersion of clusters and further opening of individual channels. The positive feedback between the membrane tension and the cluster formation hence dynamically adjusts the extent of channel clustering and their gating properties.

Next, we include the observed effect of channel clustering into our previously developed continuum model of *E. coli* cell volume recovery upon hypoosmotic shock [12]. Experimentally, we observed total cell volume expansion

within seconds after the hypoosmotic shock, followed by a period of slower, minutes-long volume recovery that exhibits a characteristic "overshoot" below the initial volume value (Fig. S12). Our continuum model explained these experimental observations by considering the change of the cellular volume (V_n) and solute concentration in time. The cell volume, and consequentially the cell membrane tension, are governed by the flux of water. Solute concentration changes are governed by the diffusive fluxes through the MSCs, enhanced by the tension build up (see the Supplemental Material [21]). Thus, when MSCs are open the solute flux through the cell membrane increases, which was described in the model with a single fitting parameter [Eq. (S10)]. To link our coarse-grained model predictions with the continuum model we now replace this single fitting parameter with a continuous function, which captures that the channel clustering (i) decreases at higher membrane tensions, (ii) decreases opening probability per channel, and (iii) increases for higher MSCs surface fractions. The introduced function hence depends on the number of channels in the cluster (N), bilayer tension (γ), and the channel surface density (ρ), and any constants are fixed by fitting to the results of the coarse-grained model [21].

We fit the experimental data on the cell volume dynamics upon hypoosmotic shock to the continuum model that captures channel clustering [Eqs. (S23)–(S24) and Fig. S12]. The fit enables us to predict the changes in the extent of MSC aggregation as the cell volume expands and recovers, Fig. 4(a). The probability of observing channels as monomers ($N = 1$) and as clusters (shown for $N = 5$) is given for each time point posthypoosmotic shock, showing that larger clusters are less likely to form at the point of maximum volume expansion (largest tension), and more likely to form as the volume recovers and the membrane tension decreases. This gives a clear prediction of our model that can be tested by imaging the extent of the channel clustering at different times posthypoosmotic shock.

To demonstrate the consequence of MSCs clustering on the cell volume recovery, we investigate what the volume dynamics would look like if the channels were prevented from clustering and if they clustered to a different extent from that in the data [Figs. 4(b) and S13]. This allows us to see that, within a specific range, channel clustering can reduce the volume "overshoot" commonly found upon recovery, without jeopardizing the channel opening at the point of maximum tension. Figures 4(b) and S14 however show that excessive clustering can lead to detrimental increase in the maximum tension in the cell envelope, suggesting that the channel clustering is finely tuned. Our prediction on the role of MSC clustering for the cell volume regulation can be probed experimentally by tracing the volume recovery posthypoosmotic shock for different extents of the clustering. The MSC clustering can be enhanced by tagging the channels with fluorescent proteins [18] or modulated by expressing the channels to different levels.

In conclusion, we showed that spontaneous aggregation of mechanosensitive membrane channels results in liquid-like clusters that exhibit lower gating activity than dispersed clusters. Our findings align well with the study by Grage *et al.* [17] in which the aggregation of *E. coli* MscLs reconstituted in lipid vesicles led to a significant decrease in the total gating activity. The patch-clamp experiments in [17] showed that a number of active channels in a patch was consistently lower than the total number of channels. These results were further reinforced by small angle neutron scattering measurements, which showed that the total membrane area increase when the channels were open is smaller than expected for independently behaving channels.

Previous continuum models suggested that, due to hydrophobic mismatch, membrane-mediated interactions between rigid, cylindrically symmetric, MSCs will lead to their collective opening [41–43]. This is not what we observe. While rigid inclusions in our model are very weakly attractive (Fig. S8), our channels can dynamically acquire different conformations. This can render membrane-mediated interactions between two channels both attractive and repulsive, possibly leading to no interactions on average. Since interactions due to hydrophobic mismatch have not been directly

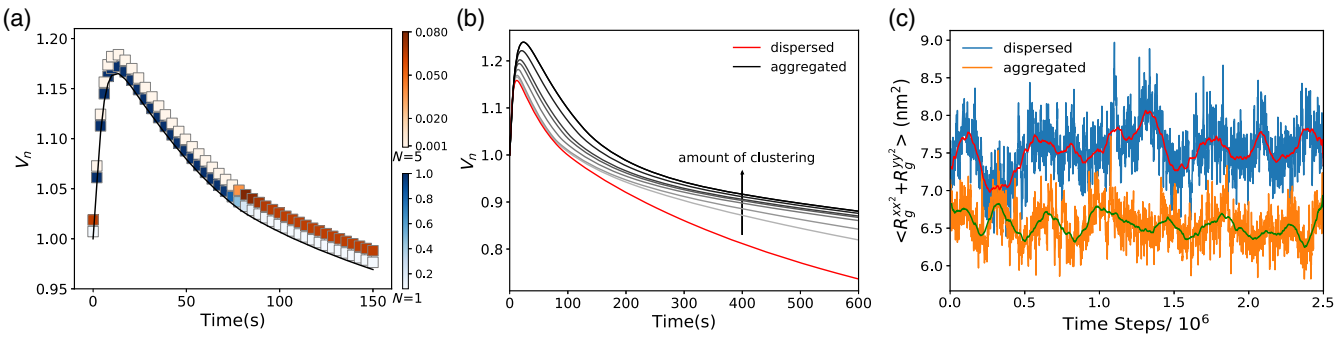

FIG. 4. Clustering regulates channel closing to prevent leaky cell membrane. (a) Normalized cell volume V_n (gray line) at 0.96 Osmol hypoosmotic shock and 0.5% channel packing fraction. Color bars: probability of finding an isolated channel (blue) and a cluster of five channels (orange). (b) Effect of increasing the extent of clustering (here by changing interprotein attractions) on cell volume dynamics (grey and black) in comparison to dispersed channels (red). Conditions as in (a). (c) The average MSC pore size at zero tension for 12 MSCs in a dispersed (blue) and aggregated (orange) states. Red and green lines show the moving time averages (10^5 steps).

experimentally quantified, it is difficult to assess their importance in driving MSC aggregation observed in experiments [17,18]. There is however a growing body of evidence that direct protein-protein interactions drive aggregation of transmembrane helices, and also stabilize helix-helix interactions within a single protein [34–39]. It is likely that the same forces could drive weak helix-helix interactions between different proteins should they find themselves close to each other.

We demonstrated that coupling between the membrane tension, channels' conformational change, and clustering produces a controlled gating system, whose positive feedback is encoded in the system's physical properties. We predict marked effects of this feedback on the cell volume regulation and suggest that MSC aggregation serves to protect the cell from excessive gating, both in a steady state and during its postshock volume recovery. Indeed, our simulations show that isolated channels have a non-zero probability of gating even at zero tension [Fig. 4(c)]. This agrees with experimental characterization of a single-channel gating that does not follow a sharp step function [44]. Hence, if MSCs are overexpressed, e.g., when bacteria grow under hyperosmotic conditions or when they enter stationary phase [45], the probability of single channel gating even under quiescent conditions would be sufficiently high to increase the effective membrane permeability to ions, making it hard to maintain electrochemical gradients across the cell membrane [30,46–50]. Furthermore, loss of volume by 8–10% leads to the loss of turgor pressure that the cell actively maintains [51]. Thus MSC aggregation, which is more pronounced at higher channel numbers, could be a natural self-defence mechanism of bacteria against unnecessary gating, contributing to bacterial survival, especially in scarce environments (alike posthypoosmotic shock). Our model identifies the basic physical mechanisms behind mechanosensing of membrane channels. Due to their generality, our results can also be helpful in guiding the design of artificial membrane channels [52,53] and synthetic nanomechanosensing systems [54].

We thank Samantha Miller, Bert Poolman, and the members of Šarić and Pilizota laboratories for useful discussions. We acknowledge support from the Engineering and Physical Sciences Research Council (A. P. and A. Š.), the UCL Institute for the Physics of Living Systems (A. P. and A. Š.), Darwin Trust of University of Edinburgh (H. S.), Industrial Biotechnology Innovation Centre (H. S. and T. P.), BBSRC Council Crossing Biological Membrane Network (H. S. and T. P.), BBSRC/EPSRC/MRC Synthetic Biology Research Centre (T. P.), and the Royal Society (A. Š.).

*a.saric@ucl.ac.uk

[1] J. L. Kavanau, Structure, and functions of biological membranes, Nature (London) **198**, 525 (1963).

[2] A. Diz-Muñoz, D. A. Fletcher, and O. D. Weiner, Use the force: Membrane tension as an organizer of cell shape and motility, Trends Cell Biol. **23**, 47 (2013).

[3] A. Anishkin, S. H. Loukin, J. Teng, and C. Kung, Feeling the hidden mechanical forces in lipid bilayer is an original sense, Proc. Natl. Acad. Sci. U.S.A. **111**, 7898 (2014).

[4] P. G. Gillespie and R. G. Walker, Molecular basis of mechanosensory transduction, Nature (London) **413**, 194 (2001).

[5] N. Eijkelkamp, K. Quick, and J. N. Wood, Transient receptor potential channels and mechanosensation, Annu. Rev. Neurosci. **36**, 519 (2013).

[6] B. Martinac, Mechanosensitive ion channels: Molecules of mechanotransduction, J. Cell Sci. **117**, 2449 (2004).

[7] E. S. Haswell, R. Phillips, and D. C. Rees, Mechanosensitive channels: What can they do and how do they do it? Structure **19**, 1356 (2011).

[8] M. D. Edwards, S. Black, T. Rasmussen, A. Rasmussen, N. R. Stokes, T.-L. Stephen, S. Miller, and I. R. Booth, Characterization of three novel mechanosensitive channel activities in Escherichia Coli, Channels **6**, 272 (2012).

[9] M. Bialecka-Fornal, H. J. Lee, and R. Phillips, The rate of osmotic downshock determines the survival probability of bacterial mechanosensitive channel mutants, J. Bacteriol. **197**, 231 (2015).

[10] C. C. Cruickshank, R. F. Minchin, A. C. Le Dain, and B. Martinac, Estimation of the pore size of the large-conductance mechanosensitive ion channel of Escherichia Coli, Biophys. J. **73**, 1925 (1997).

[11] S. I. Sukharev, W. J. Sigurdson, C. Kung, and F. Sachs, Energetic and spatial parameters for gating of the bacterial large conductance mechanosensitive channel, MscL, J. Gen. Physiol. **113**, 525 (1999).

[12] R. Buda, Y. Liu, J. Yang, S. Hegde, K. Stevenson, F. Bai, and T. Pilizota, Dynamics of Escherichia Coli's passive response to a sudden decrease in external osmolarity, Proc. Natl. Acad. Sci. U.S.A. **113**, E5838 (2016).

[13] G. Chang, R. H. Spencer, A. T. Lee, M. T. Barclay, and D. C. Rees, Structure of the MscL homolog from mycobacterium tuberculosis: A gated mechanosensitive ion channel, Science **282**, 2220 (1998).

[14] Randal B. Bass, P. Strop, M. Barclay, and D. C. Rees, Crystal structure of Escherichia Coli MscS, a voltage-modulated and mechanosensitive channel, Science **298**, 1582 (2002).

[15] E. Perozo, D. M. Cortes, P. Sompornpisut, A. Kloda, and B. Martinac, Open channel structure of MscL and the gating mechanism of mechanosensitive channels, Nature (London) **418**, 942 (2002).

[16] Y. Wang, Y. Liu, H. A. DeBerg, T. Nomura, M. T. Hoffman, P. R. Rohde, K. Schulten, B. Martinac, and P. R. Selvin, Single molecule fret reveals pore size and opening mechanism of a mechano-sensitive ion channel, eLife **3**, e01834 (2014).

[17] S. L. Grage, A. M. Keleshian, T. Turdzeladze, A. R. Battle, W. C. Tay, R. P. May, S. A. Holt, S. A. Contera, M. Haertlein, M. Moulin *et al.*, Bilayer-mediated clustering and functional interaction of MscL channels, Biophys. J. **100**, 1252 (2011).

[18] J. Van Den Berg, H. Galbiati, A. Rasmussen, S. Miller, and B. Poolman, On the mobility, membrane location and

functionality of mechanosensitive channels in Escherichia Coli, Sci. Rep. **6** (2016).
[19] P. A. Chong and J. D. Forman-Kay, Liquid–liquid phase separation in cellular signaling systems, Curr. Opin. Struct. Biol. **41**, 180 (2016).
[20] C. Maffeo, S. Bhattacharya, J. Yoo, D. Wells, and A. Aksimentiev, Modeling and simulation of ion channels, Chem. Rev. **112**, 6250 (2012).
[21] See Supplemental Material at http://link.aps.org/supplemental/10.1103/PhysRevLett.124.048102 for further details, which contains Refs. [22–28].
[22] J. D. Weeks, D. Chandler, and H. C. Andersen, Role of repulsive forces in determining the equilibrium structure of simple liquids, J. Chem. Phys. **54**, 5237 (1971).
[23] S. Plimpton, Fast parallel algorithms for short-range molecular dynamics, J. Comput. Phys. **117**, 1 (1995).
[24] W. Humphrey, A. Dalke, and K. Schulten, VMD—visual molecular dynamics, J. Mol. Graphics **14**, 33 (1996).
[25] J.-B. Fournier and C. Barbetta, Direct Calculation from the Stress Tensor of the Lateral Surface Tension of Fluctuating Fluid Membranes, Phys. Rev. Lett. **100**, 078103 (2008).
[26] Y. Deng, M. Sun, and J. W. Shaevitz, Direct Measurement of Cell Wall Stress Stiffening and Turgor Pressure in Live Bacterial Cells, Phys. Rev. Lett. **107**, 158101 (2011).
[27] E. Evans, V. Heinrich, F. Ludwig, and W. Rawicz, Dynamic tension spectroscopy and strength of biomembranes, Biophys. J. **85**, 2342 (2003).
[28] S. Kumar, J. M. Rosenberg, D. Bouzida, R. H. Swendsen, and P. A. Kollman, The weighted histogram analysis method for free-energy calculations on biomolecules. I. The method, J. Comput. Chem. **13**, 1011 (1992).
[29] I. R. Cooke, K. Kremer, and M. Deserno, Tunable generic model for fluid bilayer membranes, Phys. Rev. E **72**, 011506 (2005).
[30] S. I. Sukharev, B. Martinac, V. Y. Arshavsky, and C. Kung, Two types of mechanosensitive channels in the Escherichia Coli cell envelope: Solubilization and functional reconstitution, Biophys. J. **65**, 177 (1993).
[31] U. Schmidt, G. Guigas, and M. Weiss, Cluster Formation of Transmembrane Proteins Due to Hydrophobic Mismatching, Phys. Rev. Lett. **101**, 128104 (2008).
[32] F. de Meyer and B. Smit, Comment on "Cluster Formation of Transmembrane Proteins Due to Hydrophobic Mismatching," Phys. Rev. Lett. **102**, 219801 (2009).
[33] F. Jean-Marie De Meyer, M. Venturoli, and B. Smit, Molecular simulations of lipid-mediated protein-protein interactions, Biophys. J. **95**, 1851 (2008).
[34] D. T. Moore, B. W. Berger, and W. F. DeGrado, Protein-protein interactions in the membrane: Sequence, structural, and biological motifs, Structure **16**, 991 (2008).
[35] D. Langosch and I. T. Arkin, Interaction and conformational dynamics of membrane-spanning protein helices, Protein Sci. **18**, 1343 (2009).
[36] M. Mravic, J. L. Thomaston, M. Tucker, P. E. Solomon, L. Liu, and W. F. DeGrado, Packing of apolar side chains enables accurate design of highly stable membrane proteins, Science **363**, 1418 (2019).
[37] Y. Yano, A. Yamamoto, M. Ogura, and K. Matsuzaki, Thermodynamics of insertion and self-association of a transmembrane helix: A lipophobic interaction by phosphatidylethanolamine, Biochemistry **50**, 6806 (2011).
[38] X. Ou, P. Blount, R. J. Hoffman, and C. Kung, One face of a transmembrane helix is crucial in mechanosensitive channel gating, Proc. Natl. Acad. Sci. U.S.A. **95**, 11471 (1998).
[39] Y. Yano and K. Matsuzaki, Measurement of thermodynamic parameters for hydrophobic mismatch 1: Self-association of a transmembrane helix, Biochemistry **45**, 3370 (2006).
[40] O. Kahraman, P. D. Koch, W. S. Klug, and C. A. Haselwandter, Architecture and function of mechanosensitive membrane protein lattices, Sci. Rep. **6** (2016).
[41] T. Ursell, K. C. Huang, E. Peterson, and R. Phillips, Cooperative gating and spatial organization of membrane proteins through elastic interactions, PLoS Comput. Biol. **3**, e81 (2007).
[42] K. Guseva, Collective response of self-organised clusters of mechanosensitive channels, in *Formation and Cooperative Behaviour of Protein Complexes on the Cell Membrane* (Springer, Berlin, Heidelberg, 2012), pp. 31–67.
[43] L. D. Fernandes, K. Guseva, and A. P. S. De Moura, Cooperative response and clustering: Consequences of membrane-mediated interactions among mechanosensitive channels, Phys. Rev. E **96**, 022410 (2017).
[44] V. Belyy, K. Kamaraju, B. Akitake, A. Anishkin, and S. Sukharev, Adaptive behavior of bacterial mechanosensitive channels is coupled to membrane mechanics, J. Gen. Physiol. **135**, 641 (2010).
[45] M. Bialecka-Fornal, H. J. Lee, H. A. DeBerg, C. S. Gandhi, and R. Phillips, Single-cell census of mechanosensitive channels in living bacteria, PLoS One **7** (2012).
[46] E. Krasnopeeva, C.-J. Lo, and T. Pilizota, Single-cell bacterial electrophysiology reveals mechanisms of stress-induced damage, Biophys. J. **116**, 2390 (2019).
[47] P. Mitchell, Coupling of phosphorylation to electron and hydrogen transfer by a chemi-osmotic type of mechanism, Nature (London) **191**, 144 (1961).
[48] P. F. Costa, M. G. Emilio, P. L. Fernandes, H. G. Ferreira, and K. G. Ferreira, Determination of ionic permeability coefficients of the plasma membrane of Xenopus Laevis oocytes under voltage clamp, J. Physiol. **413**, 199 (1989).
[49] K. D. Garlid and P. Paucek, Mitochondrial potassium transport: The $k+$ cycle, Biochim. Biophys. Acta **1606**, 23 (2003).
[50] D. E. Goldman, Potential, impedance, and rectification in membranes, J. Gen. Physiol. **27**, 37 (1943).
[51] T. Pilizota and J. W. Shaevitz, Plasmolysis and cell shape depend on solute outer-membrane permeability during hyperosmotic shock in E. Coli, Biophys. J. **104**, 2733 (2013).
[52] A. R. Thomson, C. W. Wood, A. J. Burton, G. J. Bartlett, R. B. Sessions, R. L. Brady, and D. N. Woolfson, Computational design of water-soluble α-helical barrels, Science **346**, 485 (2014).
[53] K. R. Mahendran, A. Niitsu, L. Kong, A. R. Thomson, R. B. Sessions, D. N. Woolfson, and H. Bayley, A monodisperse transmembrane α-helical peptide barrel, Nat. Chem. **9**, 411 (2017).
[54] J. F. Doerner, S. Febvay, and D. E. Clapham, Controlled delivery of bioactive molecules into live cells using the bacterial mechanosensitive channel MscL, Nat. Commun. **3**, 990 (2012).